ELSEVIER

Lithos 60 (2002) 113–128

LITHOS

www.elsevier.com/locate/lithos

Abundance and distribution of PGE and Au in the island-arc mantle: implications for sub-arc metasomatism

Pavel Kepezhinskas [a,*], Marc J. Defant [b], Elisabeth Widom [c]

[a] *Geoprospects International Inc., 9302 Brookhurst Court, Tampa, FL 33647, USA*
[b] *Department of Geology, University of South Florida, Tampa, FL 33620, USA*
[c] *Department of Geology, Miami University, Oxford, OH 45056, USA*

Received 5 December 2000; accepted 17 October 2001

Abstract

Ultramafic xenoliths from a veined mantle wedge beneath the Kamchatka arc have non-chondritic, fractionated chondrite-normalized platinum-group element (PGE) patterns. Depleted (e.g., low bulk-rock Al_2O_3 and CaO contents) mantle harzburgites show clear enrichment in the Pd group relative to the Ir group PGEs and, in most samples, Pt relative to Rh and Pd. These PGE signatures most likely reflect multi-stage melting which selectively concentrates Pt in Pt–Fe alloys while strongly depleting the sub-arc mantle wedge in incompatible elements. Elevated gold concentrations and enrichment of strongly incompatible enrichment (e.g., Ba and Th) in some harzburgites suggest a late-stage metasomatism by slab-derived, saline hydrous fluids. Positive Pt, Pd, and Au anomalies coupled with Ir depletions in heavily metasomatized pyroxenite xenoliths probably reflect the relative mobility of the Pd and Ir groups (especially Os) during sub-arc metasomatism which is consistent with Os systematics in arc mantle nodules. Positive correlations between Pt, Pd, and Au and various incompatible elements (Hf, U, Ta, and Sr) also suggest that both slab-derived hydrous fluids and siliceous melts were involved in the sub-arc mantle metasomatism beneath the Kamchatka arc. © 2002 Published by Elsevier Science B.V.

Keywords: Platinum-group elements; Sub-arc metasomatism; Kamchatka arc

1. Introduction

The island-arc mantle remains one of the least documented mantle reservoirs due to the lack of mantle-wedge xenoliths brought up by arc lavas. Mantle xenoliths that may be representative of the sub arc mantle are most frequently brought to the surface by back-arc alkaline basaltic magmas (Takahashi, 1978; Brandon et al., 1996; Umino and Yoshizawa, 1996). However, mantle xenoliths also have been collected from a few arc-front localities including the Kamchatka arc, Russia (Kepezhinskas et al., 1995, 1996; Kepezhinskas and Defant, 1996), the Luzon arc, Philippines (Maury et al., 1992), and the Tabar–Lihir–Tanga–Feni (TLTF) arc, Papua New Guinea (McInnes et al., 1999). All of the mantle xenoliths from these localities display extensive modal (amphibole, phlogopite, and aluminous spinel) and cryptic (incompatible trace-element enrichments) metasomatic features which have been interpreted to be the result of reaction between a variably depleted mantle wedge and slab-derived fluids and melts (Maury et al., 1992; Kepezhinskas and Defant, 1996; McInnes et al., 1999).

Recently, Re–Os isotope systematics have been applied to address the nature of arc mantle metasoma-

* Corresponding author.
E-mail address: pkepezhi@tampabay.rr.com (P. Kepezhinskas).

0024-4937/02/$ - see front matter © 2002 Published by Elsevier Science B.V.
PII: S0024-4937(01)00073-1

tism and the origin of arc magma geochemistry. Unlike other radiogenic isotopic systems, Re and Os behave differently during mantle melting. Re is moderately incompatible, while Os is compatible during mantle melting (Martin, 1991). Brandon et al. (1996) analyzed back-arc mantle xenoliths from Simcoe (Cascades) and Ichinomegata (Japan) for Os isotopes to show that their Os isotopic characteristics are consistent with the addition of a 5–15% slab-derived component to a depleted sub-arc mantle. They further suggested that Os, along with other platinum-group elements (PGEs), can be partitioned into chlorine-rich slab fluids or melts and transported into the overlying mantle wedge (Brandon et al., 1996).

McInnes et al. (1999) showed that gold ores overlying the mantle wedge in the Tabar–Lihir–Tanga–Feni arc have Os-isotope compositions similar to those of the underlying subduction-metasomatized mantle source. Their data required the addition of a gold, copper, and PGE-enriched component to the depleted island-arc mantle to accommodate the elemental and isotopic characteristics of arc-related precious metal deposits within the arc (McInnes et al., 1999).

In addition, Widom and Kepezhinskas (1999) analyzed mantle-wedge peridotites from arc-front lavas in Kamchatka associated with the subduction of both young (northern arc segment) and old (southern arc segment) oceanic crust. They found that the Kamchatka island-arc mantle exhibits radiogenic Os signatures that are inconsistent with in-situ growth of ^{187}Os. These radiogenic Os isotopic signatures were interpreted to be the result of extensive slab melt–mantle interaction (Widom and Kepezhinskas, 1999). Although, the Os-isotope studies make a strong case for the mobility of Os during sub-arc metasomatism, the behavior of the entire suite of PGEs is still poorly understood.

Island-arc mantle xenoliths from the Kamchatka arc provide a unique opportunity to investigate metasomatism of the sub-arc mantle wedge using PGEs along with other trace-element data because of the abundance of xenoliths collected from several volcanoes and the range of metasomatic features documented. Our previous studies suggested that the southern section of the Kamchatka arc mantle undergoes a more typical metasomatism via primarily hydrous fluids whereas the subduction of relatively young crust below the northern section of the arc causes the mantle to be metasomatized via primarily siliceous melts (Kepezhinskas et al., 1995, 1996; Kepezhinskas and Defant, 1996; Widom and Kepezhinskas, 1999).

We present PGE and Au data obtained from 24 peridotitic and pyroxenitic xenoliths collected from seven volcanoes in the Kamchatka arc in order to: (1) document abundances and distribution of PGEs in a range of xenolith compositions derived from various sections of the sub-arc mantle wedge; (2) determine PGE and other trace-element signatures in island-arc mantle xenoliths related to metasomatism associated with young and hot versus old and cold slabs; (3) evaluate PGE behavior during transport from subducted crust to mantle and during subsequent slab–mantle interactions; (4) use geochemical and petrologic data from island-arc xenoliths to constrain the composition and extent of crust–mantle interactions and mantle evolution in subduction zones.

2. Geologic setting and samples

2.1. Geologic setting

The Kamchatka arc (Fig. 1) is located at the junction of the North American, Eurasian, and Pacific plates, and records a protracted history of subduction, terrane accretion, and arc volcanism. The arc can be divided into northern, central, and southern segments separated by major trunscurrent faults (Fig. 1). The southern arc segment is built upon Mesozoic–Tertiary accreted terranes, which include low-grade (greenschist) to high-grade (blueschist, amphibolite, eclogite, and granulite) metamorphic rocks of lower arc crust and subduction-zone origin. Crustal thickness beneath the southern segment of the Kamchatka arc ranges between 30 and 45 km (Kepezhinskas et al., 1997).

Fig. 1. Tectonic setting of Kamchatka arc along with major mantle xenolith locations, position of active and fossil subduction zones and trenches. Ages for the Komandorsky Basin crust and Pacific lithosphere are adopted from Bogdanov (1988). Boundary between northern and southern segments is indicated by major trunscurrent faults and crustal discontinuities (Kepezhinskas et al., 1997). The Central Kamchatka Depression marks position of an active intra-arc rift (Kepezhinskas et al., 1997).

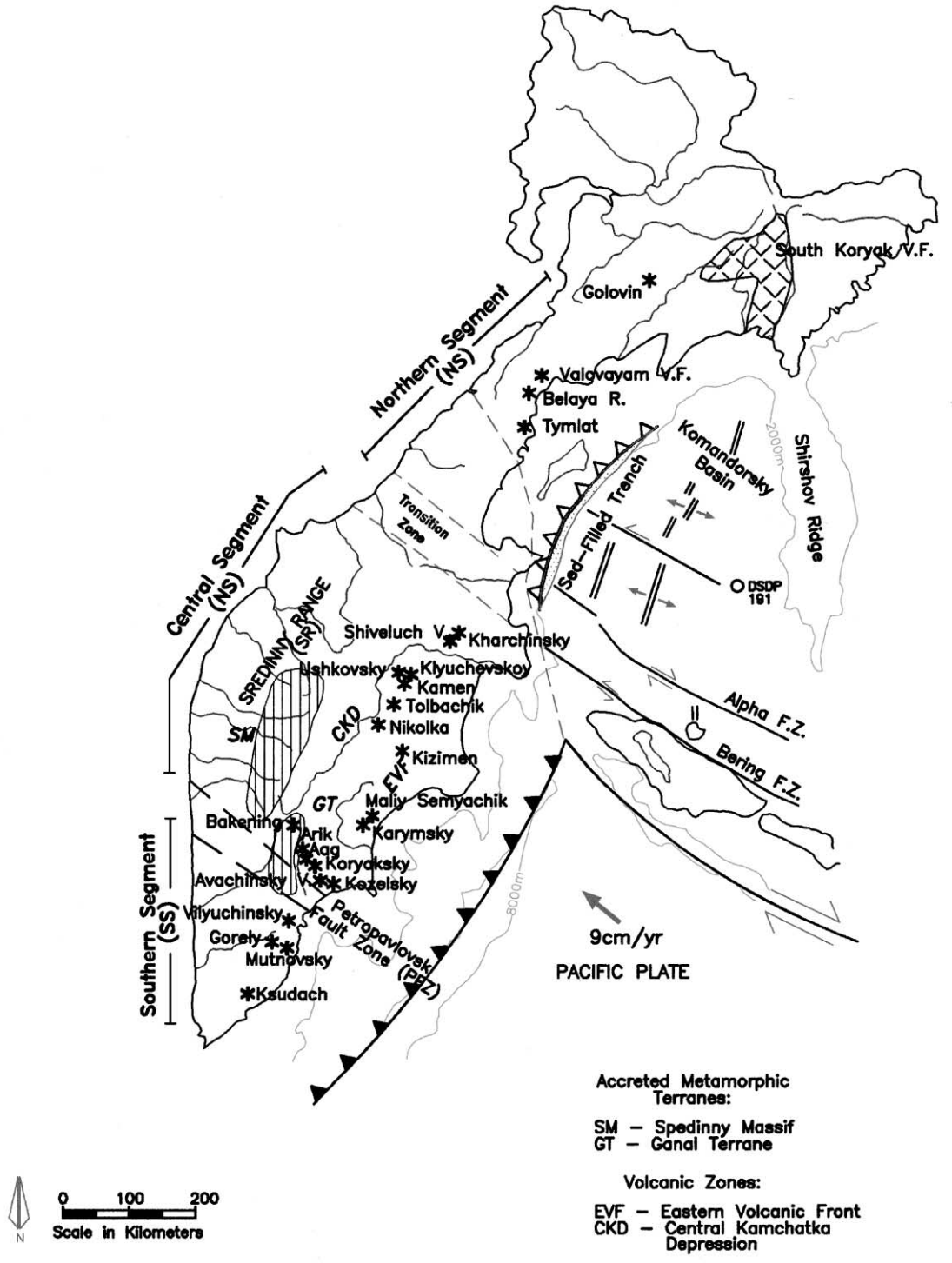
South Koryak V.F.
Golovin
Northern Segment (NS)
Valovayam V.F.
Belaya R.
Tymlat
Komandorsky Basin
Shirshov Ridge
2000m
Transition Zone
Sed-Filled Trench
DSDP 191
Central Segment (NS)
SREDINNY RANGE (SR)
Shiveluch V.
Kharchinsky
Ushkovsky
Klyuchevskoy
Kamen
Tolbachik
Nikolka
SM
CKD
EVF
Kizimen
GT
Maliy Semyachik
Bakening
Arik
Karymsky
Agg
Koryaksky
Avachinsky V.
Kozelsky
Vilyuchinsky
Gorely
Mutnovsky
Ksudach
Petropavlovsk Fault Zone (PFZ)
Southern Segment (SS)
Alpha F.Z.
Bering F.Z.
8000m
9cm/yr
PACIFIC PLATE
Accreted Metamorphic Terranes:
SM – Spedinny Massif
GT – Ganal Terrane
Volcanic Zones:
EVF – Eastern Volcanic Front
CKD – Central Kamchatka Depression
N
0 100 200
Scale in Kilometers

The northern segment of the Kamchatka arc is underlain by thickened (up to 25 km) oceanic crust composed of amphibolites, hornblende gabbros, cortlandites, and hornblende pyroxenites (Kepezhinskas et al., 1997). The segment formed in response to westward subduction of young (<25 Ma) and hot oceanic crust of the Komandorsky basin—a back-transform spreading setting (Bogdanov, 1988).

The tectonic setting of the Kamchatka arc is further complicated by active intra-arc rifting within the Central Kamchatka Depression (Fig. 1). This rift is bordered by systems of listric faults and is characterized by voluminous mafic to intermediate volcanism which includes Kluchevskoy Volcano—the largest basaltic volcanic center in Eurasia (Kepezhinskas et al., 1997).

2.2. Ultramafic xenolith suites in the Kamchatka arc

Mantle xenoliths were collected from seven volcanic centers throughout the Kamchatka arc. A total of 24 xenoliths were selected for this study based on their relatively large size, unaltered nature, and petrological variability (Kepezhinskas et al., 1995, 1996; Kepezhinskas and Defant, 1996). This xenolith suite represents along-arc and across-arc compositional variations in the sub-arc mantle wedge, which also allows us to assess potential lateral PGE heterogeneity in the island-arc mantle beneath Kamchatka.

Ultramafic xenoliths from the Kamchatka arc exhibit medium- to coarse-grained equigranular, granoblastic, porphyroclastic, and protoclastic mantle textures due to variable deformation under mantle conditions. Abundant creep-related deformational features (various tilt walls, slip bands, and polygonized microstructures frequently found in high-Mg olivines—Fo content = 90–91) and mineral defect structures (undulose olivine and kink-banded pyroxene) are consistent with derivation from the mantle wedge beneath the Kamchatka arc (Kepezhinskas et al., 1995; Kepezhinskas and Defant, 1996). These olivine microstructures are typically formed through kink nucleation, cross-slip, or climb nucleation during deformation of the peridotite xenoliths under mantle pressures and temperatures (Gueguen and Nicolas, 1980). All these microstructures indicate a residual mantle origin for the xenoliths in Kamchatka.

Two major groups are identified among Kamchatka xenoliths based upon textures and mineral composition: (1) Cr-rich spinel harzburgites, dunites, and minor lherzolites (observed only in the northern segment—Valovayam volcanic center—Fig. 1) and (2) Cr-poor spinel pyroxenites, wehrlites, and websterites with or without amphibole. Amphibole is also observed in two Cr-rich harzburgites from Avachinsky volcano. Some Cr-rich harzburgites are essentially composite nodules of the two types described above. They contain veins (1–5 cm wide) of clinopyroxenitic, orthopyroxenitic, and websteric compositions. The first group (i.e., the Cr-rich group) exhibits primary depleted mineral compositions overprinted to various degrees with cryptic and modal metasomatism. They are interpreted as primary mantle from the wedge below the arc (Kepezhinskas et al., 1995, 1996).

The second xenolith group (i.e., the Cr-poor group) is believed to be formed via progressive reaction between mantle wedge and mafic melt under mantle P–T conditions (Kepezhinskas et al., 1996). This conclusion is supported by a variety of observations including the similarity of P–T estimates for Kamchatka peridotites (T = 887–1018 °C, P = 27.4–30.5 kbar) and pyroxenites (T = 931–1043 °C, P = 27.6–30 kbar) as well as the occurrence of pyroxenites as veins in composite harzburgitic xenoliths.

Pressure and temperature estimates for Kamchatka xenoliths based on mineral and fluid inclusion thermobarometry indicate equilibration at a depth of approximately 100 km below the arc within a temperature range of 887–1043 °C (Fig. 2). The Kamchatka mantle geotherm appears to be similar to the mean oceanic geotherm at 60.4 Ma (Turcotte and Schubert, 1982) and is lower than elevated Cenozoic geotherms in eastern Australia (Sutherland et al., 1994) and the back-arc mantle environment of southwest Japan (Umino and Yoshizawa, 1996). These pressure–temperature estimates suggest that Kamchatka ultramafic xenoliths were derived from a relatively deep portion of a thermally unperturbed mantle wedge.

The Cr-rich harzburgite xenoliths are composed of olivine (75–83 modal %), orthopyroxene (15–24 modal %), clinopyroxene (0–3 modal %), and spinel (0.1–1.4 modal %). Olivine compositions are $Fo_{90-92.4}$, with NiO and Cr_2O_3 concentrations between 0.1–0.48 and 0.01–0.37 wt.%, respectively. All olivines are unzoned and have low CaO contents (<0.08 wt.%) consistent with their mantle origin. Orthopyroxene has an enstatite to ferroan enstatite

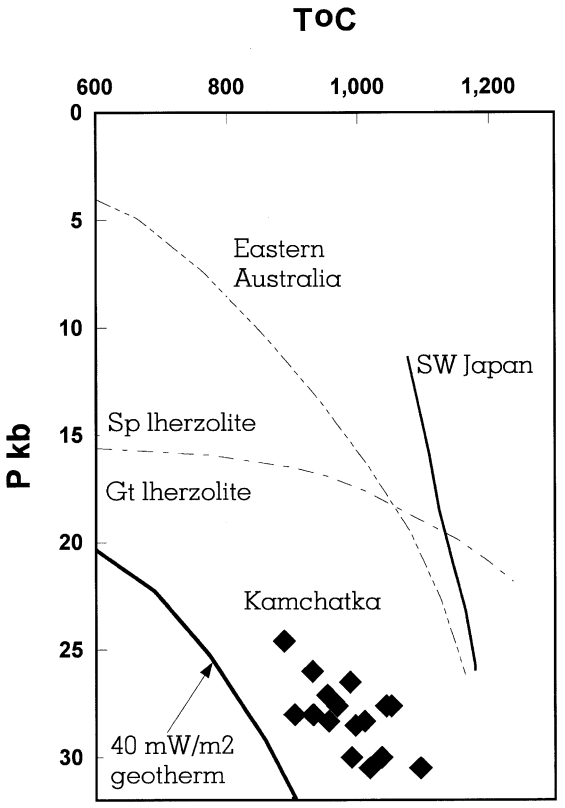

Fig. 2. Equilibration pressures and temperatures for Kamchatka ultramafic xenoliths compared with geotherms of various tectonic settings. Data sources: Eastern Australia (Sutherland et al., 1994), SW Japan (Umino and Yoshizawa, 1996). The 40 mW/m^2 shield geotherm and mean oceanic geotherm of 60.4 Ma (Turcotte and Schubert, 1982).

composition ($Wo_1En_{84-90}Fs_{9-15}$) with Al_2O_3 contents ranging from 0.4 to 1.7 wt.% and Cr_2O_3 contents between 0.2 and 0.7 wt.%. Clinopyroxene in Kamchatka xenoliths is typically diopside ($Wo_{45-47}En_{47-49}Fs_{4-8}$) with variable Cr_2O_3 concentrations (0.24–1.4 wt.%). Spinel has a Cr# (Cr/Cr+Al) of 0.53–0.77 and a Mg# (Mg/Mg+$Fe^{2+}Fe^{3+}$) of 0.48–0.60. Modal mineralogy (low modal clinopyroxene content) and refractory mineral chemistry (e.g., high Cr/Cr+Al ratios in spinels, a high Mg# in olivines and orthopyroxenes, low Al contents in orthopyroxenes, low Ti, Na, and Al and high Mg and Cr concentrations coupled with a clear LREE depletion in clinopyroxenes) reflect an overall depletion in basaltic components (Kepezhinskas et al., 1996; Kepezhinskas and Defant, 1996). In other words, the spinel harzburgite xenoliths from central Kamchatka appear to be systematically more depleted than MORB mantle in both bulk chemical and mineral compositions (Kepezhinskas and Defant, 1996).

2.3. Evidence for mantle wedge metasomatism

Ultramafic xenoliths from the northern segment of the Kamchatka arc associated with the subduction of young crust exhibit abundant textural and chemical signatures, which suggest slab melt–mantle metasomatism. These xenoliths contain three generations of clinopyroxenes with progressive enrichment in Na, Al, Sr, and light REEs (Kepezhinskas et al., 1995, 1996). The pyroxene compositional trends in northern Kamchatka xenolith suite were interpreted to be a result of slab-melt (adakite)–mantle interactions. Adakites (Defant and Drummond, 1990; Martin, 1999) are spatially and temporally associated with xenolith-bearing basaltic magmas in northern Kamchatka. The basaltic magmas also bear evidence of being derived from a source that has undergone prolific slab melt–mantle interaction (e.g., elevated MgO, Cr, and Ni contents) (Hochstaedter et al., 1996; Kepezhinskas et al., 1997). In addition, northern Kamchatka mantle xenoliths contain dacitic veins that are compositionally similar to adakites (i.e., silicic partial melts from a metabasalt) (Kepezhinskas et al., 1996). Trace-element compositions of these dacitic veins (e.g., high Sr and low Y contents coupled with high Sr/Y and La/Yb ratios) suggest metasomatism of the mantle wedge beneath northern Kamchatka by adakites (Kepezhinskas et al.,1995, 1996).

Xenoliths from the southern segment of the Kamchatka arc (produced in response to subduction of old Pacific lithosphere) contain amphibole pyroxenite, clinopyroxenite, and websterite veins that, based on their textures and *P–T* estimates, precipitated through melt–peridotite interaction. Cr-series harzburgites from southern Kamchatka exhibit detectable enrichments in LREE coupled with negative Ta and positive Ba and U anomalies on chondrite-normalized spider diagrams, signatures indicative of hydrous metasomatism (Kepezhinskas and Defant, 1996). Cr-poor wehrlitic and pyroxenitic xenoliths from southern Kamchatka have elevated Al, Na, Ba, U, and REE concentrations; all suggesting the addition of lithophile

elements to the southern Kamchatka mantle wedge by slab-derived fluids (Hochstaedter et al., 1996; Kepezhinskas and Defant, 1996).

3. Results

PGE and Au concentrations in 24 ultramafic xenoliths from the Kamchatka arc are presented in Table 1. PGE and Au analyses are by the nickel sulfide fire assay-induced coupled plasma-mass spectrometry method at X-RAL Laboratories, Toronto, Canada (Kepezhinskas and Defant, 2001). NiS fire assay was done to preconcentrate PGEs. The NiS button was dissolved in HCl and PGE phases were collected on a filter paper. Further dissolution of PGE phases was done following procedures outlined in Plessen and Erzinger (1998). Analytical errors based on analysis of standards (UMT-1, WMG-1, WMS-1 and WPR-1) and duplicates are 25% for Au, 20% for Os, and 10% for Ru, Rh, Pd, Ir and Pt (Kepezhinskas and Defant, 2001).

Harzburgite xenoliths from the arc front are found only at Avachinsky volcano and range in total PGE abundance from 25.5 ppb in sample AVX35 to 79.8 ppb in sample 1/2-91 (Table 1). Spinel lherzolite (sample 8710p) and pyroxenite (sample 8710u) nodules from the northern segment of the arc have similar concentrations of total PGEs with the exception of Ir which is six times lower in the pyroxenite (0.1 ppb) compared to the lherzolite xenolith (0.6 ppb). Both xenoliths also show elevated Au concentrations (lherzolite, 8 ppb; pyroxenite, 3 ppb) and high Au/PGE ratios (e.g., Au/Ir, 13–30; Au/Pt, 3–4; and Au/Pd, 1.5–8; Table 1) relative to most of the mantle xenoliths collected.

Os concentrations in arc-front pyroxenites are fairly constant (3–5 ppb), while Ir and Ru concentrations vary significantly (0.2–5.1 and 1–11 ppb, respectively) (Table 1). Pd-group PGEs (Rh, Pt, and Pd) also show wide variations in absolute concentrations. Pt in arc-front pyroxenite xenoliths ranges from 3 to 25 ppb, and Pd from 3 to 22 ppb. Au is slightly enriched (1–4 ppb) with the exception of wehrlitic nodule KF-52-73 (14 ppb—it is also rich in modal amphibole—10.8 modal %; Table 1).

Pyroxenite and wehrlite xenoliths from behind the arc-front volcanoes (i.e., Bakening and Kupol) have a more restricted range in their total PGEs from 17.1 to 24.4 ppb and appear to have systematically lower total PGE abundances compared to arc-front xenoliths (most of which have PGE sums of 25–78 ppb; Table 1).

Most arc-front harzburgites from Kamchatka (with the noticeable exception of heavily fractionated sample AVX35) display relatively flat C1 chondrite-normalized patterns with the exception of Pd-group metals (Pt and Pd) and Au, which appear to be fractionated one way or the other in most samples (Fig. 3A). With the exception of sample 1/2-91 which has a concave-upward PGE pattern and sample AVX35 with a sharp negative Ir anomaly (Fig. 3A), spinel harzburgites from Kamchatka have a narrow range of absolute abundances for Os, Ir, Ru, and Rh (0.006–0.015×C1 chondrite) in comparison with the extreme variations in Pt, Pd, and Au absolute concentrations (0.002 to 0.243×C1 chondrite). This argues against the "nugget effect" control on PGE distribution in analyzed samples due to heterogeneous distribution of PGE-carrying minerals in the Kamchatkan mantle. It suggests the importance of Pt-bearing alloys for PGE behavior in arc peridotites. This is further supported by the extreme rarity of sulphides and PGE alloys among minerals in Kamchatka spinel harzburgites. Our detailed microprobe studies detected only two pentlandite grains among 168 microprobed opaque minerals in 14 arc-front harzburgitic xenoliths (Kepezhinskas et al., 1996; Kepezhinskas and Defant, 1996; Kepezhinskas and Defant, unpublished data).

Pyroxenitic veins in composite harzburgite xenoliths from arc-front lavas have mildly fractionated PGE patterns (Fig. 3B) with slight but clear increase in chondrite-normalized concentrations from the Ir group (Os, Ir, and Ru, 0.002–0.015×C1 chondrite) to Pd group (Rh, Pt, and Pd, 0.008–0.038×C1 chondrite) as well as positive Pd and Pt anomalies. Discrete pyroxenitic nodules from arc-front volcanoes (AVX47 and KF-52-73 from Avachinsky; KOZ-XM-D from Kozelsky; and SH-1 from Sheveluch volcanoes) have strongly fractionated chondrite-normalized patterns with significant fractionation between both Ir- and Pd-group PGEs (Fig. 3C). Pd-group PGEs are also fractionated: sample SH-1 has a clear positive Pt anomaly while amphibole pyroxenite (AVX47) and wehrlite (KF-52-73) samples from Avachinsky volcano exhibit similar chondrite-normalized patterns

Table 1
PGE and Au results. Abundance of platinum-group element (PGE) and Au in mantle xenoliths from the Kamchatka arc

Volcano	Sample	Lithology	Os (ppb)	Ir (ppb)	Ru (ppb)	Rh (ppb)	Pt (ppb)	Pd (ppb)	Au (ppb)	Pt/Pd	Pt/Pt*	$(Pt/Ir)_N$	$(Pd/Ir)_N$	$(Ru/Ir)_N$	$(Au/Ir)_N$	$(Pt/Os)_N$
Arc front xenoliths																
Avachinsky	AVX5	Sp-harzburgite	3	3	4	1	12	4	1	3.00	1.92	1.70	1.00	0.86	1.00	2.00
	AVX8	Sp-harzburgite	3	2.6	11	1	12	5	1	2.40	1.95	2.00	1.52	2.50	1.17	2.00
	AVX33	Sp-harzburgite	6	4.5	10	2	10	7	1	1.43	0.86	1.00	1.30	1.40	0.70	0.83
		duplicate	5	4.4	9	2	11	7	1.4	1.57	0.94	1.10	1.30	1.30	1.00	1.10
	AVX35	Sp-harzburgite	3	0.5	2	1	17	2	6.1	8.50	3.84	17.00	4.00	3.00	44.00	2.83
	AVX51	Sp-harzburgite	4	3.4	7	1	7	10	3	0.70	0.71	1.00	2.57	1.43	3.00	0.88
	AVX37	Sp-harzburgite	3	4.4	5	2	26	3	2.9	8.67	3.40	2.57	0.78	0.70	2.10	4.33
		duplicate	3	4.3	7	2	23	3	1	7.67	3.00	2.30	0.55	1.00	0.80	3.83
	AVX45	Sp-harzburgite	3	3.4	8	1	19	3	3.5	6.30	3.51	2.70	0.78	1.57	3.57	3.14
	AVX48	Sp-harzburgite	4	3.2	7	2	9	16	34	0.56	0.51	1.27	4.16	1.43	34.70	1.13
	AVX49	Sp-harzburgite	3	2.3	15	1	7	1	7	7.00	2.24	1.40	0.36	4.20	10.00	1.17
	1/2-91	Sp-harzburgite	3	6.8	28	3	29	10	0.8	2.90	1.69	1.91	1.21	2.60	0.40	4.79
		duplicate	3	5.6	23	2	31	9	1	3.44	2.34	2.56	0.46	2.67	0.58	5.12
	AVX47	Amph pyroxenite	3	0.3	2	1	3	3	2.5	1.00	0.55	3.00	5.45	2.82	18.00	1.82
	KF-52-73	Amph wehrlite	4	0.3	2	2	11	11	14	1.00	0.75	11.00	20.00	2.82	100.00	1.98
	AVX36-V	Pyroxenite vein	3	1.3	3	1	16	11	2	1.46	2.41	5.28	6.67	1.41	4.67	2.26
	AVX34-V	Pyroxenite vein	3	0.9	3	1	12	3	1	4.00	2.21	5.94	2.73	2.11	3.50	1.70
	AVX44-V	Pyroxenite vein	3	4.7	11	3	25	21	1	1.19	1.01	2.48	3.82	1.40	0.70	3.54
		duplicate	3	5.1	10	3	24	22	1	1.09	0.94	2.16	3.64	1.28	0.64	3.40
Kozelsky	KOZ-XM-D	Pyroxenite	4	0.2	2	1	10	12	3	0.83	0.92	24.75	21.82	3.52	52.50	1.25
		Duplicate	5	0.3	4	1	12	14	4	0.86	1.03	11.88	25.45	5.63	32.22	1.20
Sheveluch	SH-1	Amph pyroxenite	3	0.4	1	1	16	3	1	5.33	2.95	15.84	5.00	1.28	6.36	2.26
Valovayam	8710p	Sp-lherzolite	4	0.6	2	1	2	1	8	2.00	0.64	1.98	1.65	2.17	47.50	0.25
	8710u	Sp-pyroxenite	3	0.1	1	1	1	2	3	0.50	0.23	4.95	18.18	7.04	105.00	0.14
Navarin	30-90	Sp-lherzolite	7	1.3	5	1	4	5	2	0.80	0.57	1.32	3.03	2.35	4.68	0.28
Behind-the-arc-front xenoliths																
Bakening	48-54	Sp-pyroxenite	9	0.4	3	1	4	7	12	0.57	0.48	3.96	11.57	3.84	78.18	0.22
		duplicate	7	0.3	3	1	2	6	11	0.33	0.26	2.05	10.91	4.23	79.00	0.14
	48-4	Sp-pyroxenite	8	0.1	2	1	3	6	12	0.50	0.39	14.85	54.55	14.09	428.57	0.19
	48-108	Sp-pyroxenite	3	0.1	1	1	12	1	1	12.00	3.84	59.40	9.10	7.05	35.00	1.70
		duplicate	3	0.1	1	1	10	2	1	5.00	2.26	49.50	18.18	7.05	35.00	1.40
Kupol	Kup 17-1	Wehrlite	3	1.9	2	1	12	2	1	6.00	2.71	2.97	0.91	0.70	1.75	1.70

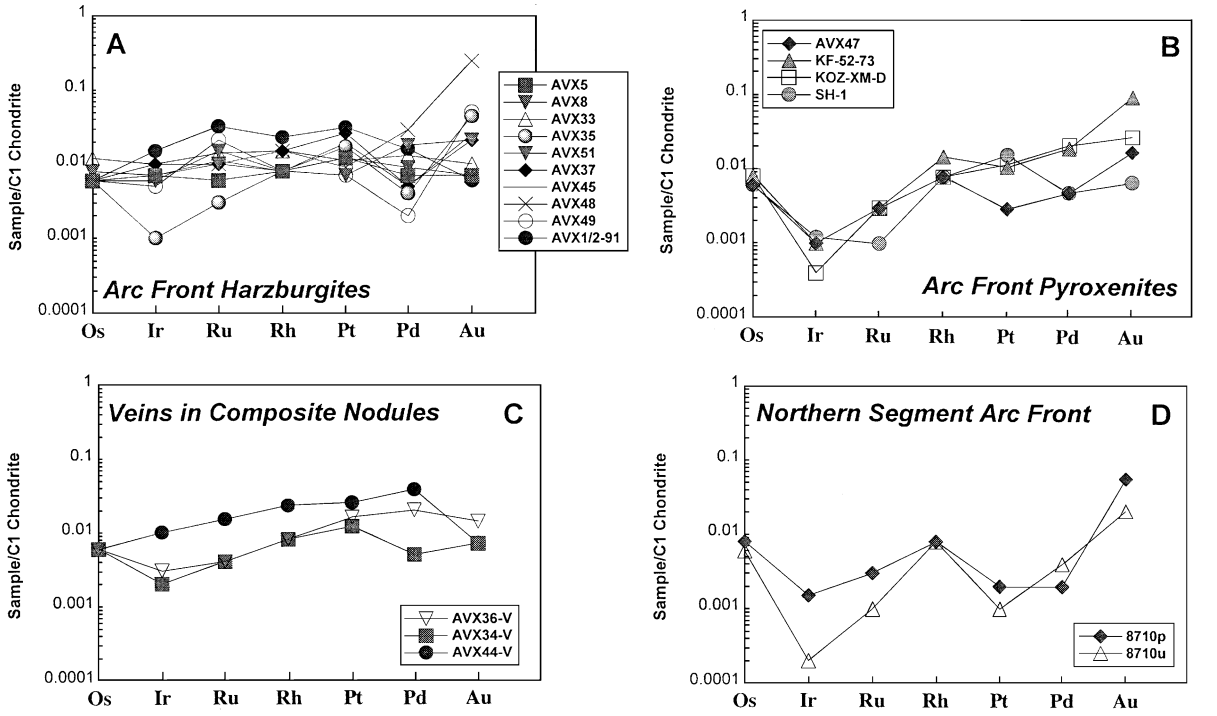

Fig. 3. Chondrite-normalized noble metal patterns for harzburgites (A), pyroxenites (B), pyroxenitic veins in composite xenoliths (C) and north segment lherzolite/pyroxenite (D) from arc front lavas in Kamchatka. Normalizing values for C1 chondrite are from McDonough and Sun (1995).

with a weak negative Pt anomaly and a clear enrichment in Au relative to the PGEs (Fig. 3C). Lherzolite (8710p) and pyroxenite (8710u) from the northern-arc segment (associated with young crust subduction) have very low absolute concentrations of all noble metals (0.001–0.008×C1 chondrite) except Au (0.057×C1 and 0.021×C1 chondrite, respectively) and Ir in sample 8710p (0.015×C1 chondrite) coupled with fractionated normalized patterns (Fig. 3D). Both samples display a weak negative Pt anomaly similar to most arc-front pyroxenite xenoliths from Kamchatka.

Pyroxenite xenoliths from Bakening volcano (located behind the arc, see Fig. 1) have fractionated chondrite-normalized patterns with a strong negative Ir anomaly (Fig. 4). Two pyroxenite xenoliths (48-54 and 48-4) display negative Pt anomalies, while sample 48-108 from Bakening and wehrlite xenolith Kup 17-1 from Kupol volcano have positive Pt anomalies similar to Pt enrichments in arc-front harzburgites (Figs. 3A and 4). The wehrlite xenolith from Kupol volcano has the least fractionated normalized pattern with a weak depletion in Ru relative to Os and Ir and a weak depletion in Pd relative to Pt and Au (Fig. 4).

These fractionations among the Pd-group PGEs are also documented by elevated Pt/Pd ratios in Kamchatka harzburgites, which range from 0.56 to 8.67

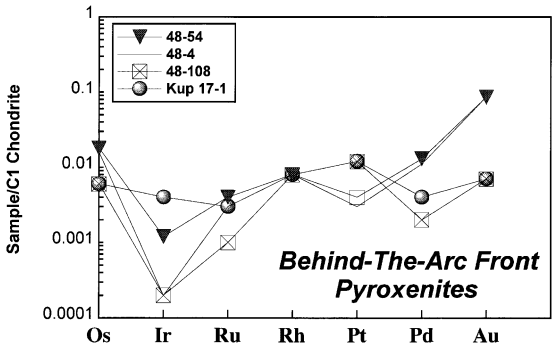

Fig. 4. Chondrite-normalized noble metal patterns for pyroxenite and wehrlite xenoliths from the behind-the-arc-front lavas. Normalizing values for C1 chondrite are from McDonough and Sun (1995).

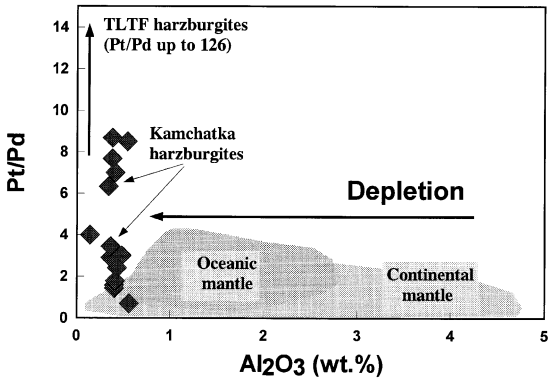

Fig. 5. Pt/Pd versus Al_2O_3 (wt.%) in continental mantle (Gueddari et al., 1996; Garuti et al., 1997b; Pattou et al., 1996), oceanic mantle (Rehkamper et al., 1999; Snow and Schmidt, 1998) and harzburgitic mantle xenoliths from Papua New Guinea (McInnes et al., 1999) compared to Kamchatka mantle wedge peridotites (filled diamonds).

with an average of 4.17 (Table 1, Fig. 5). Only three samples exhibit sub-chondritic Pt/Pd ratios of <2 (the chondritic Pt/Pd ratio ranges from 1.4 to 2; Table 2 and McDonough and Sun, 1995; Snow and Schmidt, 1998; Jagoutz et al., 1979; Morgan, 1986). The platinum enrichment relative to other Pd-group PGEs in most sub-arc harzburgites from Kamchatka can be further demonstrated using a Pt/Pt* parameter, or Pt anomaly, suggested originally by Garuti et al. (1997a). The Pt anomaly ($Pt/Pt^*=Pt_N/Rh_N\times Pd_N$) provides a measure of the deviation of Pt concentration from the general trend of the primitive mantle-normalized pattern of a sample. Primitive unfractionated mantle has a Pt/Pt* value of 1 (Barnes et al., 1988; Garuti et al., 1997a). Three spinel harzburgites from the Kamchatka arc—AVX 33, AVX51, and AVX48—display negative Pt anomalies ranging from 0.51 to 0.94 (Table 1, Fig. 6), while the rest of the analyzed mantle wedge xenoliths (seven samples) have positive Pt anomalies (1.69–3.84, average = 2.07) (Table 1). Kamchatka harzburgites also display enrichment in $(Pt/Os)_N$ (1.13–4.79; average = 2.55) and $(Pt/Ir)_N$ (1.00–17.00; average = 2.96) ratios with the exception of the same, slightly Pt-depleted samples AVX33 (0.83 and 1.00, respectively) and AVX51 (0.70 and 1.00, respectively). All these data suggest that, with the exception of chondritic to sub-chondritic Pd-group PGE patterns in samples AVX33, AVX51, and AVX48, the rest of mantle wedge peridotites from the Kamchatka arc display non-chondritic ratios with clear Pt enrichment.

Arc-front pyroxenites show a range in Pt/Pt* ratios from negative (0.55–0.94; Table 1) to positive (2.2–2.95) ratios. Pyroxenites with both positive and negative Pt anomalies show clear enrichments in the Pd group and Au relative to the Ir group (Ir and Os): (Pt/

Table 2
Average composition of island-arc mantle compared to other mantle reservoirs. Average concentrations of platinum-group elements and gold in C1 chondrite, model pyrolite, primitive mantle continental lithospheric mantle, oceanic mantle, Tabar–Lihir–Tanga–Feni harzburgites, Alaskan-type ultramafic complexes and Kamchatka Island-arc mantle peridotites

	C1 model	Pyrolite	PM1	PM2	CLM	OCM	TLTF	AUC	KAM
Ru (ppb)	710	5.0	4.3	5.6	12.4	6.04	1.83	2.22	10.46
Rh (ppb)	130	0.9	2.4	1.6			4.37	4.73	1.62
Pd (ppb)	550	3.9	4	4.4	3.9	5.88	3.29	33.65	6.15
Os (ppb)	490	3.4	3.3	4.2	4		3.9	3.23	3.54
Ir (ppb)	455	3.2	3.3	4.4	3.7	3.43	1.01	4.89	3.72
Pt (ppb)	1010	7.1	7	8.3	7	7.81	32.5	86.5	16.39
Au (ppb)	140	1.0	0.5	1.2	0.65		0.72	8.32	4.9
Pt/Pd	1.84	1.82	1.75	1.89	1.80	1.33	9.88	3.89	4.17
Pt/Os	2.06	2.09	2.12	1.98	1.75		8.33	42.57	5.44
Au/Pd	0.26	0.26	0.13	0.27	0.17		0.22	0.27	0.21
$(Ru/Ir)_N$		1.00	0.86	0.80	2.13	1.14	1.50		1.90
$(Pt/Ir)_N$		1.00	1.00	1.00	0.88	1.03	16.09		2.96
$(Pd/Ir)_N$		1.00	1.00	0.80	0.88	1.44	3.00		1.54

Data sources: C1 model, pyrolite, primitive mantle (PM1) and continental lithospheric mantle (CLM) are from Mcdonough and Sun (1995). Primitive mantle 2 (PM2) estimate is from Barnes et al. (1988). Oceanic mantle (OM) is from Rehkamper et al. (1999). Average for Tabar–Lihir–Tanga–Feni (TLTF) harzburgite xenoliths is after McInnes et al. (1999). Alaskan-type ultramafic–mafic complexes (AUC) average is a compilation of data from Garuti et al. (1997a). Kamchatka mantle xenoliths (KAM) from this study.

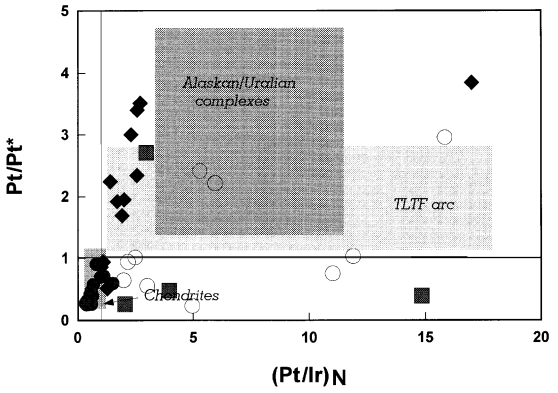

Fig. 6. Pt/Pt* (Pt anomaly) versus $(Pt/Ir)_N$ in harzburgites (filled diamonds), arc front pyroxenites (open circles) and behind-the-front pyroxenites (filled squares) from Kamchatka arc compared to harzburgites from Papua New Guinea (McInnes et al., 1999), orogenic lherzolites (filled circles; Garuti et al., 1997b; Pattou et al., 1996; Barnes et al., 1985; Lorand, 1989) and Uralian/Alaskan zoned ultramafic–mafic complexes (Garuti et al., 1997a; Loney and Himmelberg, 1992; Nixon et al., 1997). The Pt anomaly ($Pt/Pt^* = Pt_N/Rh_N \times Pd_N$) provides a measure of the deviation of Pt concentration from the general trend of the primitive mantle-normalized pattern of a sample. Primitive unfractionated mantle has a Pt/Pt* value of 1 (Barnes et al., 1988; Garuti et al., 1997a). Positive ($Pt/Pt^* > 1$) or negative ($Pt/Pt^* < 1$) anomalies indicate Pt fractionation from Rh and Pd as a result of different petrologic processes. Primitive mantle normalizing values for Pt, Rh and Pd (Pt anomaly) are from Barnes et al. (1988). C1 chondrite normalizing values for Pt and Ir (Pt/Ir ratio) are from McDonough and Sun (1995).

$Ir)_N$, 2–24.75; $(Pd/Ir)_N$, 2.7–25.45; (Au/Ir), 3–105; and $(Pt/Os)_N$, 1.2–3.5 (Table 1). Arc-front pyroxenites plot either at sub-chondritic or above-chondritic Pt/Pt* values in Fig. 6, but also at systematically higher $(Pt/Ir)_N$ values reflecting strong Ir depletions in the pyroxenitic component of the veined mantle wedge.

Lherzolite and pyroxenite nodules from the northern arc segment have negative Pt/Pt* anomalies of 0.64 and 0.23 coupled with an overall enrichment of Pd-group PGEs and, especially, Au relative to Ir: $(Pt/Ir)_N$, 1.98 and 4.95; $(Pd/Ir)_N$, 1.65 and 18.2; and (Au/Ir), 47.5 and 105. Low Pt concentrations in the northern segment xenoliths are also reflected in the low $(Pt/Os)_N$ ratios of 0.25 and 0.14.

Pyroxenite xenoliths from behind-the-front volcanoes can be sub-divided into two groups on the basis of fractionations among and between the Ir- and Pd-group PGEs. The low-Pt group (samples 48-54 and 48-4 from Bakening volcano) display negative Pt anomalies (Pt/Pt* values of 0.26–0.48; Table 1) coupled with low Pt/Pd (0.33–0.57), low $(Pt/Os)_N$ (0.14–0.22), and high $(Au/Ir)_N$ (78–428) ratios. The high-Pt group PGEs (samples 48-108 from Bakening and Kup 17-1 from Kupol volcanoes) have positive Pt anomalies (Pt/Pt* values of 2.26–3.84; Table 1) coupled with high Pt/Pd (5–12), high $(Pt/Os)_N$ (1.4–1.7), and relatively low $(Au/Ir)_N$ (1.75–35) ratios. This subdivision is further emphasized by the dual distribution of behind-the-front pyroxenites in Fig. 6. As in the case of arc-front pyroxenites, both Pt enrichments and depletions relative to other Pd-group metals are coupled with clear Pt enrichments relative to Ir.

4. Discussion

Both residual and metasomatic xenoliths from the Kamchatka arc show clear fractionation among various PGEs and Au. Overall, the Pd group appears to be enriched relative to the Ir group in all Kamchatkan mantle-wedge xenoliths. The two major trends in noble metal abundances and distribution in the island-arc mantle beneath Kamchatka appear to be predominant Pt enrichment in residual harzburgites (Cr-rich xenolith group) and variable fractionation of Au, Pt, and Pd with consistent enrichment of the Pd group over Ir group in pyroxenites (Cr-poor group), in most xenoliths combined with extreme depletions in Ir.

In order to evaluate the significance of the PGE systematics in island-arc mantle, we have further attempted to compare our data with mantle peridotites from other tectonic environments to decide on the implications for metasomatic processes in the sub-arc mantle wedge.

4.1. Comparisons with mantle peridotites from different tectonic settings

Average PGE and Au concentrations and some key element ratios for Kamchatka and for Tabar–Lihir–Tanga–Feni (TKTF, Papua New Guinea) mantle, as well as C1 chondrite, primitive mantle, continental lithospheric mantle, and oceanic mantle are summarized in Table 2. The mantle wedge beneath the TKTF arc appears to be similar to the Kamchatka island-arc mantle in the non-chondritic, fractionated distribution

of Pd-group PGEs. In fact, TKTF peridotites exhibit one of the highest Pt/Pd ratios (up to 126.5; Fig. 5) with an average Pt/Pd ratio of 9.88 (Table 2) and $(Pt/Ir)_N$ ratios of up to 18.6. In comparison, primitive mantle estimates from McDonough and Sun (1995) and Barnes et al. (1988) have Pt/Pd ratios of 1.75 and 1.89, respectively. Also, primitive mantle has $(Pt/Ir)_N$ ratios of 1.0, continental lithospheric mantle of 0.88, and oceanic mantle of 1.03 (Table 2). Most orogenic lherzolites and CLM spinel lherzolite xenoliths from alkaline basalts plot close to or within the chondrite field in Fig. 6. Pt is clearly enriched in island-arc mantle from both TKTF and Kamchatka relative to the Ir-group PGE.

One of the important chemical features of the island-arc mantle is its overall depletion in lithophile elements such as Al and Ca (Bonatti and Michael, 1989; Maury et al., 1992; Brandon et al., 1996; Kepezhinskas and Defant, 1996). Spinel harzburgites from the Kamchatka arc have low Al_2O_3 (0.34–0.66 wt.%) and CaO (0.40–0.78 wt.%) contents consistent with their depleted residual nature of the mantle due to multiple melt extraction (Kepezhinskas and Defant, 1996). Kamchatka mantle xenoliths plot on the depleted end of the mantle array in a $Pt/Pd–Al_2O_3$ graph and also show clear enrichments in Pt (Pt/Pd ratios up to 8.67). In contrast, both continental mantle (on the basis of an orogenic peridotite database, Garuti et al., 1997b; Pattou et al., 1996) and oceanic mantle have higher Al (and Ca) contents and, with the exception of a single dunite sample from ODP hole 895E in the Hess Deep, eastern Pacific Ocean (Pt/Pd ratio of 3.99, sample 895E 6R1 51-56 in Table 1 of Rehkamper et al., 1999), have systematically lower Pt/Pd ratios compared to island-arc peridotites from Kamchatka and TKTF (Fig. 5).

This is further emphasized by chondrite-normalized PGE patterns for average mantle compositions from different environments. Primitive mantle, as well as continental lithospheric mantle, has essentially flat patterns with chondritic or slightly sub-chondritic values for the Pd-group PGE (0.007–0.012×C1 chondrite; Pattou et al., 1996; Rehkamper et al., 1997). Oceanic mantle (Rehkamper et al., 1999) also seems to have a flat PGE pattern. Oceanic mantle has an absolute Pd concentration similar to the Kamchatka island-arc mantle—0.011×C1 chondrite—however, normalized Pt concentrations in Kamchatka peridotites (0.018×C1 chondrite) are clearly higher than that of the average oceanic mantle (0.008×C1 chondrite). Both Kamchatka and TKTF mantle averages have non-chondritic, fractionated Pd-group PGE patterns with a clear positive Pt anomaly and, in the case of Kamchatka mantle, a positive Au anomaly (Table 2).

The depleted nature of island-arc mantle compared to CLM and oceanic mantle is also reflected in relatively high Os concentrations and very low Re/Os ratios (Fig. 7). Harzburgites from Kamchatka and TKTF plot on the most depleted end of the mantle restite compositions (Re/Os ratios of < 0.03) comparable to the most depleted cratonic harzburgites from the Kaapvaal. In fact, Kamchatka harzburgites have Re concentrations much lower than the most depleted upper mantle (Widom and Kepezhinskas, 1999). This testifies to a protracted history of depletion by removal of partial melts in the Kamchatka mantle wedge, which has dramatic implications for PGE systematics for the island-arc mantle in general.

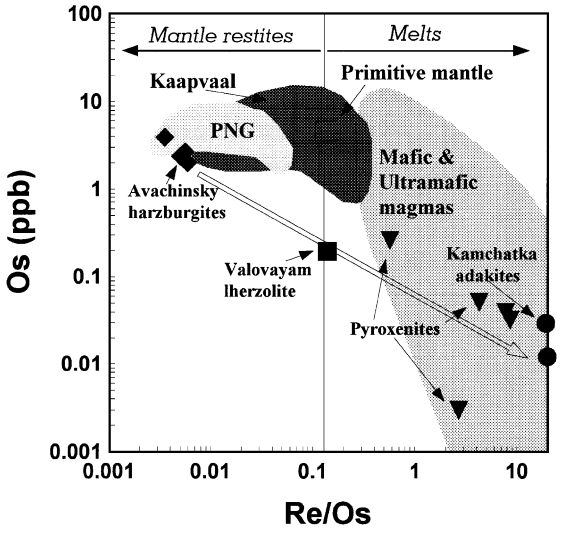

Fig. 7. Re/Os versus Os concentrations in ultramafic xenoliths from Kamchatka arc. Avachinsky peridotites=closed circles, Avachinsky pyroxenites (veins in two composite xenoliths)=closed diamonds. Filled fields represent sub-arc mantle wedge xenoliths from the Tubaf seamount in the Papua New Guinea arc system (McInnes et al., 1999), Kaapvaal craton peridotites (Walker et al., 1989) and a compilation of ocean–island basalts and komatiites representing mantle-derived mafic and ultramafic magmas (Martin, 1991; Hauri and Hart, 1997; Reisberg et al., 1993; Widom and Shirey, 1996; Walker et al., 1989). Chondritic and primitive mantle values (filled circle) are from Morgan (1986).

4.2. Origin of Pt enrichment in island-arc mantle

One of the most striking characteristics of depleted island-arc mantle appears to be its enrichment in Pt relative to Pd (McInnes et al., 1999; this study). Selective fractionation of Pt from Pd distinguishes arc mantle from other mantle environments, such as primitive mantle, continental lithospheric mantle (orogenic lherzolite or spinel lherzolite xenolith estimates), and oceanic mantle. Although many mantle peridotites have somewhat fractionated patterns, the origin of which is a subject of a debate in the recent literature (this goes beyond the scope of the current paper, but see Pattou et al., 1996; Rehkamper et al., 1997, 1999 for summaries), sharp non-chondritic Pt enrichments in mantle wedge xenoliths are so well defined that this geochemical signature deserves special consideration.

Simple mantle fractionation under peculiar chemical–physical conditions fails to easily explain selective separation of Pt from Rh and Pd. For example, similar f_S conditions in the chromitite-forming system in ophiolitic peridotites cause formation of Ir–Os–Ru alloys, not Pt–Fe alloys, which are capable of fractionating Pt from Pd and Rh (Fleet and Stone, 1991). Similarly, sulphide segregation or precipitation during partial melting or melt–peridotite interaction in the mantle is an unlikely decoupling mechanism since Pt and Pd partition coefficients between silicate and sulphide liquids are similar (Peach et al., 1990). It has been suggested by Garuti et al. (1997a,b) that extraction of melt(s) from a mantle source can leave refractory Pt–Fe alloys in the residue selectively enriching the residual mantle source in Pt. As suggested by the slightly elevated Pt/Pd ratios in oceanic mantle peridotites (Pt/Pd ratios of 0.80–3.99; Rehkamper et al., 1999), a single episode of melt extraction beneath mid-ocean ridge is not sufficient to fractionate Pt from the rest of Pd-group PGEs. Additional melt extraction episodes are potentially required to generate this unique non-chondritic PGE signature. Extensive isotopic and trace-element studies of primitive arc magmas indicate that at least a two-stage melting process in a back-arc–basin–volcanic arc system is required for the remarkable depletion in lithophile elements inferred for arc mantle sources (Woodhead et al., 1993; Ewart and Hawkesworth, 1987; Hochstaedter et al., 1996). Similar multi-stage melting is probably required for effective separation of Pt from other PGEs via Pt alloy accumulation in residual arc-mantle sources.

This is consistent with CaO and PGE co-variations in depleted harzburgite xenoliths from Kamchatka, as illustrated in Fig. 8. Progressive melting (defined by the melting trend in Fig. 8) will lead to a slight increase in Pt/Pd ratios from a fertile upper mantle with 3.2–4.0 wt.% CaO to a depleted upper mantle with CaO of less than 1 wt.%. However, in the case of the Kamchatka mantle wedge, Pt/Pd ratios increase dramatically when very depleted mantle compositions are reached (0.3–0.8 wt.% CaO). This increase in Pt/Pd ratios in severely depleted mantle requires formation of a refractory mineral phase, which will concentrate Pt exclusively at the expense of Pd. Pt–Fe alloys seem to be the best fit for such a phase. Accessory Pt–Fe alloys are documented in mantle sections of suprasubduction zone ophiolites as well as in accreted mantle peridotite fragments in modern arcs (Leblanc, 1991). Ir seems to follow the same behavior as shown in Fig. 8C. Progressive melting decreases CaO and slightly increases Ir concentrations in mantle peridotites. As in the case of the Pt/Pd ratio, increases occur in Ir concentrations at very low CaO contents in Kamchatka mantle wedge peridotites (Fig. 8C). This increase in Ir concentrations is coupled with an increase in Ru concentrations, which likely reflects formation of a residual Ir–Ru alloy, such as laurite, during advanced multi-stage melting. In any case, these fractionations seem to be best explained by the formation of residual Pt and, to a lesser extent Ru–Ir, alloys during progressive melting of the primitive mantle. This model is consistent with other trace-element characteristics of island-arc mantle such as its profound depletion in a range of incompatible elements which suggest multiple melt extractions prior to metasomatism by slab-derived fluids (Maury et al., 1992; Woodhead et al., 1993; Hochstaedter et al., 1996).

4.3. Constraints from PGE systematics on sub-arc metasomatism

Pyroxenitic xenoliths from Kamchatka typically have fractionated chondrite-normalized noble-metal patterns with predominant enrichment in Pd-group PGEs and Au relative to the Ir group. Pd-group metals, in most cases, show further fractionation within the

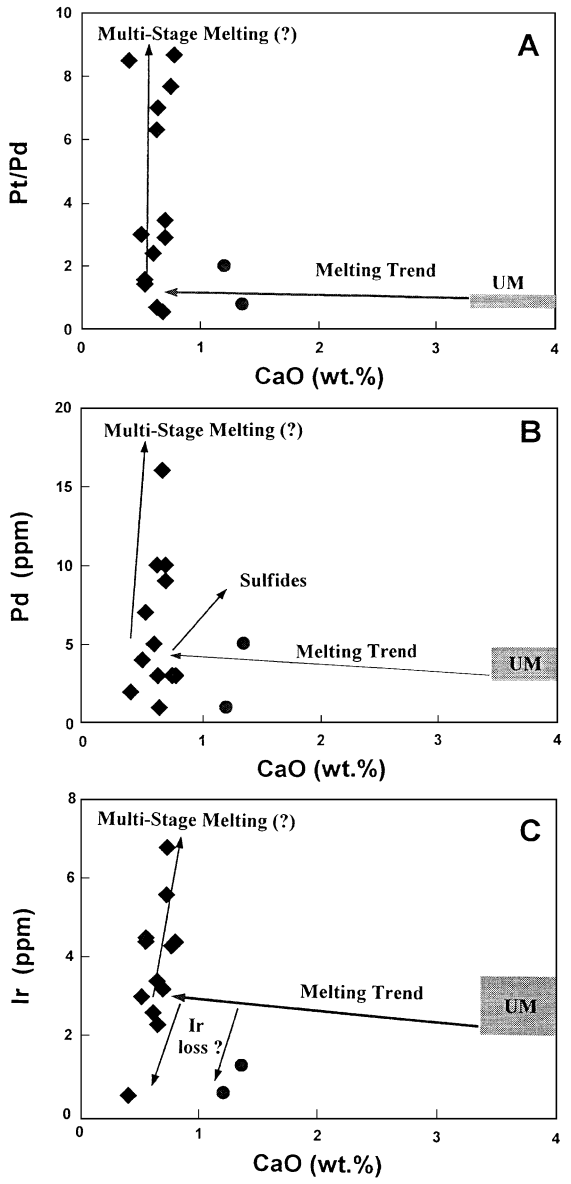

Fig. 8. Variation of Pt/Pd ratio (A), Pd (B) and Ir (C) concentrations versus CaO in Kamchatkan harzburgites (filled diamonds) and lherzolites (filled circles). The Melting Trend shows the PGE trends for progressive depletion of a fertile upper mantle (UM) by magma extraction following the melting model of Rehkamper et al. (1999). The PGE concentrations and ratios for fertile upper mantle (UM) are after McDonough and Sun (1995). Sulfide addition trends refer to refertilization of variably depleted mantle residues by basaltic melts (see Rehkamper et al., 1999 for details). The low Ir abundances in some harzburgites and lherzolites from sub-arc mantle may be due to the depletion of this element by secondary processes.

group with some pyroxenite nodules showing clear enrichment in Pt relative to Rh and Pd (positive Pt/Pt* anomaly and high Pt/Pd ratios) and other xenoliths displaying Pd and Au enrichments (negative Pt/Pt* anomaly, low Pt/Pd, and high Au/Pt and Au/Pd ratios). This compositional variability probably reflects different conditions of equilibration with residual mantle during formation of pyroxenites as well as a range in slab-derived components involved in sub-arc metasomatism.

Another striking feature of pyroxenite xenoliths from Kamchatka is the consistent depletion in Ir relative to Os and Ru (Figs. 3B and 4). This Ir depletion supports the metasomatic origin of pyroxenites via magmatic crystallization under mantle-wedge conditions, because most melts contain very low concentrations of this metal (Barnes et al., 1985, 1988). This pronounced Ir depletion in arc pyroxenite xenoliths may also indicate relative mobility of Os in the sub-arc mantle. Our preliminary $^{187}Os/^{188}Os$ isotope data for Kamchatka as well as previously published results from Japan and the Cascades (Brandon et al., 1996) suggest that Os can be mobile in the presence of slab-derived hydrous fluids. Kamchatka harzburgite and lherzolite xenoliths show a correlation between a decreasing Os/Ir ratio and increasing Au/Pt ratio, suggesting that sub-arc metasomatism via fluid–mantle interaction can decrease Os/Ir ratios significantly below sub-chondritic values. Since Os and Ir show a reasonable positive correlation, it appears that both metals can be mobile during sub-arc metasomatism by slab-derived hydrous fluids.

Fig. 7 illustrates continuous decrease in Os concentrations and Re/Os ratios from harzburgites through lherzolite (i.e., 8710p to pyroxenites). Kamchatka pyroxenites plot within the field of ultramafic/mafic magmas and on a continuous trend from depleted mantle peridotites to slab melts (adakites). This compositional trend may reflect metasomatism of depleted mantle wedge by slab melts during formation of pyroxenitic veins. Olivine will break down during adakite–mantle interaction resulting in formation of orthopyroxene along with precipitation of clinopyroxene, amphibole, and aluminous spinel (Sen and Dunn, 1995; Drummond et al., 1996). All these phases are present in pyroxenite xenoliths from Kamchatka (Kepezhinskas et al., 1995, 1996; Kepezhinskas and Defant, 1996). Adakite veins with Sr/Y of 290 were

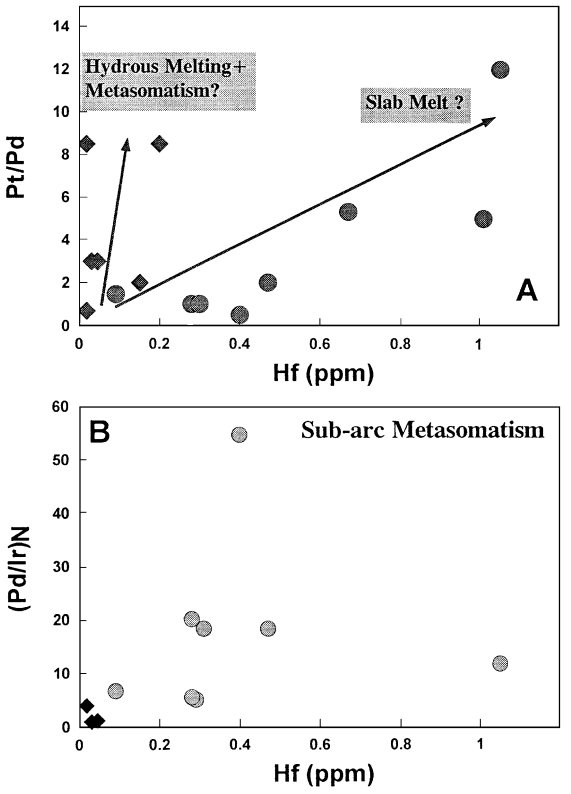

Fig. 9. Variation of (A) Pt/Pd and (B) $(Pd/Ir)_N$ ratios versus Hf concentrations in harzburgitic (filled diamonds) and pyroxenitic (filled circles) xenoliths from the Kamchatka arc. Hf data by instrumental neutron activation (J.L. Joron, analyst).

reported from lherzolite xenoliths from the northern Kamchatka arc front which is associated with subduction of young oceanic crust (Kepezhinskas et al., 1996).

Unlike hydrous fluids, slab-derived melts (adakites) are capable of carrying high-field strength elements (HFSE) such as Hf, Nb, and Ta (Defant and Drummond, 1990; Drummond et al., 1996; Martin, 1999). This distinct geochemical signature potentially can be passed on to a mantle wedge upon extensive slab melt–mantle interaction. Our PGE and other trace-element data suggest that such interaction indeed occurred beneath both the northern and southern segments of the Kamchatka arc. Positive correlations between Pt/Pd and $(Pd/Ir)_N$ ratios and Hf concentrations in Kamchatka xenoliths indicate the involvement of slab melt in sub-arc mantle metasomatism (Fig. 9). Since hydrous fluids do not carry any substantial concentrations of Hf, coupled enrichments in Pd relative to Ir and Pt relative to Pd along with an increase in Hf concentrations suggest that slab melt–mantle interactions are capable of fractionating Pt and Pd from Ir-group metals along with fractionating of HFSE from other incompatible elements. Au shows distinctly different behavior (Fig. 10). Increase in Au concentrations does not appear to correlate with an increase in Hf concentrations in the Kamchatka xenoliths (Fig. 10A), which could be interpreted as a result of adakite–mantle interaction. In fact, all xenoliths with high Hf concentrations have fairly low Au contents of less than 2 ppb. Co-variation between Au and Ta mimics this picture. All xenoliths with high Au contents are Ta-poor (Fig. 10B). Since Au is soluble in hydrous fluids, gold behavior in Kamchatka xenoliths reflects metasomatism by hydrous fluids, rather then melts.

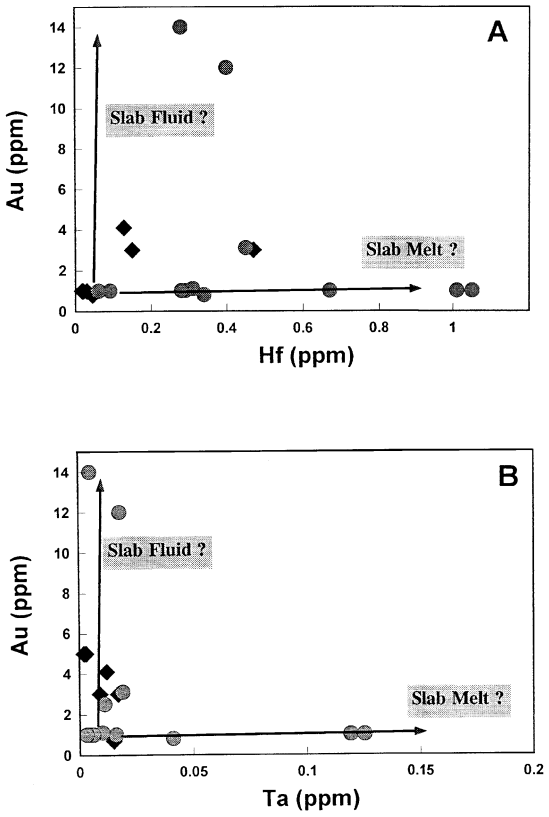

Fig. 10. Variation of Au versus (A) Hf and (B) Ta in peridotitic (filled diamonds) and pyroxenitic (filled circles) xenoliths from the Kamchatka arc. Hf and Ta data by instrumental neutron activation (J.L. Joron, analyst).

PGE and Au systematics in Kamchatka ultramafic xenoliths combined with other petrographic (presence of amphibole, Al-rich spinel, and metasomatic glasses enriched in Na, Al, Sr, and light REE) and geochemical (enrichment in HFSE such as Hf, and LILE such as U) data are consistent with extensive sub-arc metasomatism beneath both segments of the Kamchatka arc by slab-derived hydrous fluids and siliceous melts (adakites).

5. Conclusions

Peridotite and pyroxenite xenoliths representing different parts of the veined mantle wedge have non-chondritic, fractionated PGE patterns. Depleted (low Al_2O_3 and CaO contents) harzburgites show clear enrichment in the Pd group over the Ir group, coupled in most samples with Pt enrichment relative to Rh and Pd (positive Pt/Pt* anomalies and high Pt/Pd ratios). These PGE signatures most probably reflect multi-stage melting and selective concentration of Pt by Pt–Fe alloys in a severely depleted sub-arc mantle wedge. Elevated Au contents (up to 6.1 ppb) in some harzburgites suggest metasomatism by slab-derived, saline hydrous fluids. This is consistent with the presence of pyroxenitic veins in some composite xenoliths as well as some lithophile trace-element (Ba and Th, in particular) enrichments in harzburgites documented earlier by Kepezhinskas and Defant (1996).

Island-arc mantle has PGE abundances and distributions, which are distinctly different from mantle peridotites from different tectonic settings (primitive mantle, continental lithospheric mantle, and oceanic mantle). These compositional differences most likely reflect a multi-stage melting history and re-fertilization of island-arc mantle by slab-derived fluids and melts.

Pyroxenite xenoliths from island-arc mantle show highly fractionated PGE patterns with enrichments in Pt, Pd, and Au relative to the Ir group, coupled with well-pronounced Ir depletions. These anomalies probably reflect relative mobility of the Pd group as well as the Ir group (especially Os and Ir) metals during sub-arc metasomatism, which is consistent with Os systematics in island-arc mantle nodules (Brandon et al., 1996; Widom and Kepezhinskas, 1999). Positive correlations between PGE concentrations and ratios (Pt/Pd, Pd/Ir, Au/Ir, etc.) and trace-element contents (Hf, U, Ta, Sr, etc.) indicate that both slab-derived hydrous fluids and siliceous melts were involved in sub-arc mantle metasomatism beneath the Kamchatka arc.

References

Barnes, S.J., Naldrett, A.J., Gorton, M.P., 1985. The origin of the fractionation of platinum-group elements in terrestrial magmas. Chem. Geol. 81, 45–53.

Barnes, S.J., Boyd, R., Korneliusson, A., Nilsson, L.P., Often, M., Pedersen, R.B., Robins, B., 1988. The use of mantle normalization and metal ratios in discriminating between the effects of partial melting, crystal fractionation and sulphide segregation on platinum-group elements, gold, nickel and copper: examples from Norway. In: Prichard, H.M., Potts, P.J., Bowles, J.F.W., Cribb, S.J. (Eds.), Geo-Platinum 87. Elsevier, London, pp. 113–143.

Bogdanov, N.A., 1988. Geology of the Komandorsky deep basin. J. Phys. Earth 36, 65–71.

Bonatti, E., Michael, P.J., 1989. Mantle peridotites from continental rifts to ocean basins to subduction zones. Earth Planet. Sci. Lett. 91, 297–311.

Brandon, A.D., Creaser, R.A., Shirey, S.B., Carlson, R.W., 1996. Osmium recycling in subduction zones. Science 272, 861–864.

Defant, M.J., Drummond, M.S., 1990. Derivation of some modern arc magmas by melting of young subducted lithosphere. Nature 347, 662–665.

Drummond, M.S., Defant, M.J., Kepezhinskas, P., 1996. The petrogenesis of slab derived trondhjemite–tonalite–dacite/adakite magmas. Trans. R. Soc. Edinburgh: Earth Sci. 87, 205–216.

Ewart, A., Hawkesworth, C.J., 1987. The Pleistocene–Recent Tonga–Kermadec arc lavas: interpretation of new isotopic and rare earth data in terms of a depleted source model. J. Petrol. 28, 495–530.

Fleet, M.E., Stone, W.E., 1991. Partitioning of platinum-group elements in the Fe–Ni–S system and their fractionation in nature. Geochim. Cosmochim. Acta 55, 245–253.

Garuti, G., Fershtater, G., Bea, F., Montero, P., Pushkarev, E.V., Zaccarini, F., 1997a. Platinum-group elements as petrological indicators in mafic–ultramafic complexes of the central and southern Urals: preliminary results. Tectonophysics 276, 181–194.

Garuti, G., Oddone, M., Torres-Ruiz, J., 1997b. Platinum-group-element distribution in subcontinental mantle: evidence from the Ivrea Zone (Italy) and the Betic–Rifean Cordillera (Spain and Morocco). Can. J. Earth Sci. 34, 444–456.

Gueddari, K., Piboule, M., Amosse, J., 1996. Differentiation of platinum-group elements (PGE) and of gold during partial melting of peridotites in the lherzolitic massifs of the Betic–Rifean range (Ronda and Beni Bousera). Chem. Geol. 134, 181–197.

Gueguen, P., Nicolas, A., 1980. Deformation of mantle rocks. Ann. Rev. Earth Planet. Sci. 8, 119–144.

Hauri, E., Hart, S.R., 1997. Rhenium abundances and systematics in oceanic basalts. Chem. Geol. 139, 185–205.

Hochstaedter, A.G., Kepezhinskas, P.K., Defant, M.J., Drummond, M.S., Koloskov, A., 1996. Insights into the volcanic arc mantle wedge from magnesian lavas from the Kamchatka arc. J. Geophys. Res. 101, 697–712.

Jagoutz, E., Palme, H., Baddenhausen, H., Blum, K., Cendales, M., Dreibus, G., Spettel, B., Lorenz, V., Wanke, H., 1979. The abundances of major, minor and trace elements in the Earth's mantle as derived from primitive ultramafic nodules. Proc. Lunar Planet. Sci. Conf. 10, 2031–2050.

Kepezhinskas, P., Defant, M.J., 1996. Contrasting styles of mantle metasomatism above subduction zones: constraints from ultramafic xenoliths in Kamchatka. Geophys. Monogr. AGU 96, 307–313.

Kepezhinskas, P.K., Defant, M.J., 2001. Nonchondritic Pt/Pd ratios in arc mantle xenoliths: evidence for platinum enrichment in depleted island-arc mantle sources. Geology 29, 851–854.

Kepezhinskas, P.K., Defant, M.J., Drummond, M.S., 1995. Na metasomatism in the island-arc mantle by slab melt–peridotite interaction: evidence from mantle xenoliths in the North Kamchatka arc. J. Petrol. 36, 1505–1527.

Kepezhinskas, P.K., Defant, M.J., Drummond, M.S., 1996. Progressive enrichment of island arc mantle by melt–peridotite interaction inferred from Kamchatka xenoliths. Geochim. Cosmochim. Acta 60, 1217–1229.

Kepezhinskas, P., McDermott, F., Defant, M.J., Hochstaedter, A., Drummond, M.S., Hawkesworth, C.J., Koloskov, A., Maury, R.C., Bellon, H., 1997. Trace element and Sr–Nd–Pb isotopic constraints on a three-component model of Kamchatka arc petrogenesis. Geochim. Cosmochim. Acta 61, 577–600.

Leblanc, M., 1991. Platinum-group elements and gold in ophiolitic complexes: distribution and fractionation from mantle to ocean floor. In: Peters, T.J., Nicolas, A. (Eds.), Ophiolite Genesis and Evolution of the Oceanic Lithosphere, Kluwer. pp. 231–260.

Loney, R.A., Himmelberg, G.R., 1992. Petrogenesis of Pd-rich intrusion at Salt Chuck, Prince of Wales Island: an Early Paleozoic Alaskan-type ultramafic body. Can. Mineral. 30, 1005–1022.

Lorand, J.P., 1989. Abundance and distribution of Cu–Fe–Ni sulfides, sulfur, copper and platinum-group elements in orogenic-type spinel lherzolite massifs of Ariege (Northeastern Pyrenees, France). Earth Planet. Sci. Lett. 93, 50–64.

Martin, C.E., 1991. Os isotopic characteristics of mantle derived rocks. Geochim. Cosmochim. Acta 55, 1421–1434.

Martin, H., 1999. Adakitic magmas: modern analogues of Archean granitoids. Lithos 46, 411–429.

Maury, R.C., Defant, M.J., Joron, J.-L., 1992. Metasomatism of the sub-arc mantle inferred from trace elements in Philippine xenoliths. Nature 360, 661–663.

McDonough, W.F., Sun, S.-S., 1995. The composition of the Earth. Chem. Geol. 120, 223–253.

McInnes, B.I.A., McBride, J.S., Evans, N.J., Lambert, D.D., Andrew, A.S., 1999. Osmium isotope constraints on ore metal recycling in subduction zones. Science 286, 512–516.

Morgan, J., 1986. Ultramafic xenoliths: clues to Earth's late accretionary history. J. Geophys. Res. 91, 12375–12387.

Nixon, G.T., Hammack, J.L., Ash, C.H., Cabri, L.J., Case, G., Connelly, J.N., Heaman, L.M., La Flamme, J.H.G., Nuttall, C., Paterson, W.P.E., Wong, R.H., 1997. Geology and platinum-group mineralization of Alaskan-type ultramafic–mafic complexes in British Columbia. B. C. Minist. Employ. Investment, Bull. 93.

Pattou, L., Lorand, J.P., Gros, M., 1996. Non-chondritic platinum-group element ratios in the Earth's mantle. Nature 379, 712–715.

Peach, L.C., Mathez, E.A., Keyas, R.R., 1990. Sulfide melt–silicate melt distribution coefficients for noble metals and other chalcophile elements as deduced from MORB: implication for partial melting. Geochim. Cosmochim. Acta 54, 3379–3389.

Plessen, H.G., Erzinger, J., 1998. Determination of the platinum-group elements and gold in twenty rock reference samples by inductively coupled plasma-mass spectrometry (ICP-MS) after pre-concentration by nickel sulfide fire assay. Geostand. Newsl. 22, 187–194.

Rehkamper, M., Halliday, A.N., Barford, D., Fitton, J.G., Dawson, J.B., 1997. Platinum-group element abundance patterns in different mantle environments. Science 278, 1595–1598.

Rehkamper, M., Halliday, A.N., Alt, J., Fitton, J.G., Zipfel, J., Takazawa, E., 1999. Non-chondritic platinum-group element ratios in oceanic mantle lithosphere: petrogenetic signature of melt percolation? Earth Planet. Sci. Lett. 172, 65–81.

Reisberg, L., Zindler, A., Marcantonio, F., White, W., Wyman, D., Weaver, B., 1993. Os isotope systematics in ocean island basalt. Earth Planet. Sci. Lett. 120, 149–167.

Sen, C., Dunn, T., 1995. Experimental modal metasomatism of a spinel lherzolite and the production of amphibole-bearing peridotite. Contrib. Mineral. Petrol. 119, 394–409.

Snow, J.E., Schmidt, G., 1998. Constraints on Earth accretion deduced from noble metals in the oceanic mantle. Nature 391, 166–169.

Sutherland, F.L., Raynor, L.R., Pogson, R.E., 1994. Spinel to garnet lherzolite transition in relation to high temperature paleogeotherms, eastern Australia. Aust. J. Earth Sci. 41, 205–220.

Takahashi, E., 1978. Petrologic model of the crust and upper mantle of the Japanese island arcs. Bull. Volcanol. 41, 529–547.

Turcotte, D.L., Schubert, G., 1982. Geodynamics: Applications of Continuum Physics to Geological Problems Wiley 450 pp.

Umino, S., Yoshizawa, E., 1996. Petrology of ultramafic xenoliths from Kishyuku Lava, Fukue-jima, southwest Japan. Contrib. Mineral. Petrol. 124, 154–166.

Walker, R.J., Carlson, R.W., Shirey, S.B., Boyd, F.R., 1989. Os, Sr, Nd, and Pb isotope systematics of southern Africa peridotite xenoliths: implications for the chemical evolution of subcontinental mantle. Geochim. Cosmochim. Acta 53, 1583–1595.

Widom, E., Kepezhinskas, P., 1999. Osmium isotope systematics in Kamchatka arc mantle xenoliths: implications for mantle–slab fluid interactions. EOS 80, S354.

Widom, E., Shirey, S.B., 1996. Os isotope systematics in the Azores: implications for mantle plume sources. Earth Planet. Sci. Lett. 142, 451–465.

Woodhead, J., Eggins, S., Gamble, J., 1993. High field strength and transition element systematics in island arc and back-arc basin basalts: evidence for multi-phase melt extraction and a depleted mantle wedge. Earth Planet. Sci. Lett. 114, 491–504.